



HAL
open science

Constraining the landscape of Late Bronze Age Santorini prior to the Minoan eruption: Insights from volcanological, geomorphological and archaeological findings

Dávid Karátson, Tamás Telbisz, Ralf Gertisser, Thomas Strasser, Paraskevi Nomikou, Timothy Druitt, Viktor Vereb, Xavier Quidelleur, Szabolcs Kósik

► To cite this version:

Dávid Karátson, Tamás Telbisz, Ralf Gertisser, Thomas Strasser, Paraskevi Nomikou, et al.. Constraining the landscape of Late Bronze Age Santorini prior to the Minoan eruption: Insights from volcanological, geomorphological and archaeological findings. *Journal of Volcanology and Geothermal Research*, 2020, 401, pp.106911. 10.1016/j.jvolgeores.2020.106911 . hal-02926160

HAL Id: hal-02926160

<https://hal.science/hal-02926160>

Submitted on 31 Aug 2020

HAL is a multi-disciplinary open access archive for the deposit and dissemination of scientific research documents, whether they are published or not. The documents may come from teaching and research institutions in France or abroad, or from public or private research centers.

L'archive ouverte pluridisciplinaire **HAL**, est destinée au dépôt et à la diffusion de documents scientifiques de niveau recherche, publiés ou non, émanant des établissements d'enseignement et de recherche français ou étrangers, des laboratoires publics ou privés.



Distributed under a Creative Commons Attribution 4.0 International License



Constraining the landscape of Late Bronze Age Santorini prior to the Minoan eruption: Insights from volcanological, geomorphological and archaeological findings

Dávid Karátson^{a,*}, Tamás Telbisz^a, Ralf Gertisser^b, Thomas Strasser^c, Paraskevi Nomikou^d, Timothy Druitt^e, Viktor Vereb^{a,e}, Xavier Quidelleur^f, Szabolcs Kósik^g

^a Department of Physical Geography, Faculty of Sciences, Eötvös University, Budapest, Hungary

^b School of Geography, Geology and the Environment, Keele University, Keele, UK

^c Department of Art and Art History, Providence College, Providence, RI, USA

^d Faculty of Geology and the Geoenvironment, National and Kapodistrian University of Athens, Athens, Greece

^e Laboratoire Magmas et Volcans, Université Clermont Auvergne-CNRS-IRD, Clermont-Ferrand, France

^f GEOPS, Université Paris-Sud, CNRS, Université Paris-Saclay, Orsay, France

^g Volcanic Risk Solutions, Institute of Agriculture and Environment, Massey University, Palmerston North, New Zealand

ARTICLE INFO

Article history:

Received 4 December 2019

Received in revised form 29 April 2020

Accepted 5 May 2020

Available online 11 May 2020

ABSTRACT

One of the best known places on Earth where volcanology meets archaeology and history is the volcanic island of Santorini (Thíra), Greece. It is famous for the cataclysmic Late Bronze Age (Minoan) Plinian eruption which destroyed the Minoan culture that flourished on the island. Hosting a central, flooded caldera bay and, within that, the active islands of Palaea and Nea Kameni, Santorini volcano has been the focus of international research efforts for over one and a half centuries. In this paper, we summarize recent findings and related ideas about the Minoan physiography of the island, also known as Strongyli, from a volcanological, geomorphological and archaeological point of view. As proposed as early as the 1980s, a central caldera bay existed prior to the Late Bronze Age. Probably characterised by a smaller size and located in the northern part of the present-day caldera, this earlier caldera bay was formed during the previous Plinian eruption – called Cape Riva eruption – c. 22,000 years ago. Within the caldera bay, a central island, Pre-Kameni, existed, named after the present-day Kameni Islands. High-precision radioisotopic dating revealed that Pre-Kameni started to grow c. 20,000 years ago. Whereas volcanologists have accepted and refined the caldera concept, archaeologists have generally favoured the theory of an exploded central cone instead of a pre-existing central caldera. However, analysis of the Flotilla Fresco, one of the wall paintings found in the Bronze Age settlement of Akrotiri, reveals the interior of a Late Bronze Age caldera that may be interpreted as a realistic landscape. Approximately 3600 years ago, the island of Strongyli was destroyed during the explosive VEI = 7 Minoan eruption. Pre-Kameni was lost by this eruption, but its scattered fragments, together with other parts of Strongyli, can be recovered as lithic clasts from the Minoan tuffs. On the basis of photo-statistics and granulometry of the lithic clasts contained in the Minoan tuffs, complemented by volumetric assessment of the erupted tephra and digital elevation model (DEM) analysis of alternative models for the pre-eruptive topography, the volume of Pre-Kameni can be constrained between 1.6 and 3.0 km³, whereas the volume of the destroyed portion of the ring island of Strongyli between 9.1 and 17.1 km³. Of these, the larger values are considered more realistic, and imply that most of the destroyed part of Strongyli was incorporated as lithic components in the Minoan tuffs, whereas up to 3 km³ of Strongyli might have been downfaulted and sunken during caldera formation and is not accounted for in the lithics.

© 2020 The Authors. Published by Elsevier B.V. This is an open access article under the CC BY-NC-ND license (<http://creativecommons.org/licenses/by-nc-nd/4.0/>).

Contents

1. Introduction	2
2. The Late Bronze Age (Minoan) eruption: timing, processes and products	2

* Corresponding author.

E-mail address: dkarat@ludens.elte.hu (D. Karátson).

3.	Constraining the volume of the destroyed parts of Strongyli and Pre-Kameni on the basis of the lithic clast content	5
4.	Evolution of the interpretation of the Late Bronze Age landscape.	7
5.	Discussion	7
5.1.	The pre-existing caldera as shown by archaeological evidence	7
5.2.	Towards reconstructing the topography of Strongyli prior to the Minoan eruption	10
6.	Conclusions.	12
	Declaration of competing interest	12
	Acknowledgments	12
	References.	12

1. Introduction

Santorini (also known as Thira), the southernmost island of the Cyclades in the Aegean Sea, is best known to geologists and archaeologists for its Late Bronze Age Minoan culture (Marinatos, 1967–1974) and the VEI = 7 eruption that destroyed it (e.g., Bond and Sparks, 1976; Friedrich et al., 1988; Druitt et al., 1999; Johnston et al., 2014). According to Herodotus, the island at that time was named Strongyli (“The round one” in Greek) for its circular shape (not to be confused with two present-day Strongyli islands in the Eastern Mediterranean). After the Minoan eruption, the Phoenicians called the island Kallisto (“The most beautiful” in Greek); later on, the main island became known as Thera, named by the Phoenician commander Theras. The present name of Santorini was given by the Venetians in the 13th century in reference to Saint Irene. Present-day Santorini consists of the arcuated, largest island of Thira (as spelt in modern Greek) and the smaller islands of Thirasia and Aspronisi, encompassing the central Kameni islands, which have formed subsequent to the Minoan eruption (Fig. 1).

In this paper, we expand on our previous findings presented at the 10th Cities on Volcanoes conference (CoV10) in Naples, Italy (Karátson et al., 2018a) and published in Karátson et al. (2018b). Our main objective, by synthesizing and discussing published and new volcanological, geomorphological and archaeological data, is to assess how the topography of the Minoan Strongyli island can be reconstructed.

2. The Late Bronze Age (Minoan) eruption: timing, processes and products

Santorini is one out of five volcanic fields (Sousaki; Aegina-Methanaporos; Milos; Christiana-Santorini-Kolumbo; Kos-Nisyros-Yali) representing the Plio-Quaternary Aegean Volcanic arc (e.g., Fytikas and Vougioukalakis, 2005; Nomikou et al., 2013), the activity of which has been mainly controlled by the northward subduction of the oceanic segment of the African plate under the Aegean part of the continental Eurasian plate (Fig. 2; e.g., Papazachos and Comninakis, 1971; Spakman et al., 1988; Bocchini et al., 2018). The volcanic activity of



Fig. 1. Aerial photograph of Santorini from northeast (credit: Tom Pfeiffer, www.volcanodiscovery.com/santorini_i49059). Kameni Islands are to the left. The flooded central bay corresponds to the northern part of the present-day caldera, which already existed in the Late Bronze Age, whereas the southern part of the caldera (faintly visible behind the Kamenis) as well as the entrances in the west and north may have been formed during the Minoan eruption ~1630–1600 BCE.

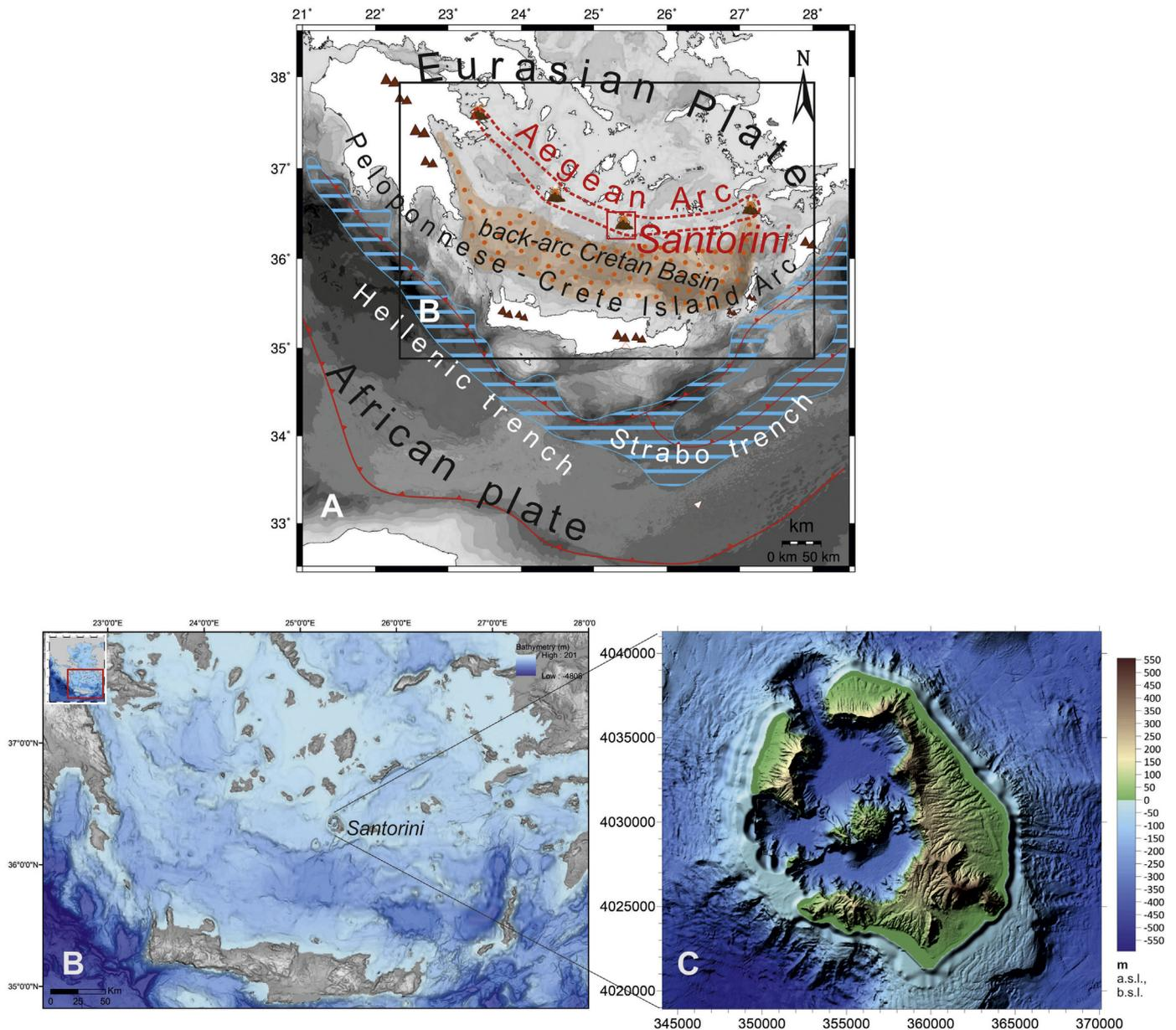


Fig. 2. Geodynamic setting of the Hellenic Arc (a) and the onshore-offshore synthetic topography of Santorini and its surroundings (b) in the South Aegean (modified from Nomikou et al., 2013); shaded, coloured DEM image of present-day Santorini (c), modified from Nomikou et al. (2014, 2016) and Karátson et al. (2018b).

Santorini, producing a wide range of basaltic to rhyolitic magmas of mostly calc-alkaline character, developed in the past c. 650 kyrs, and shifted to highly explosive, cyclic eruptive behaviour c. 360 ka ago (Druitt et al., 1999). Over this period, at least twelve Plinian eruptions have been identified, which were related to the extended generation and then rapid upward pulses of intermediate to silicic magmas resulting in the formation of at least four calderas (Druitt et al., 1989, 1999, 2016; Gertisser et al., 2009; Flaherty et al., 2018). Two of the largest caldera-forming eruptions, the so-called Lower Pumice 2 (c. 177 ka; Wulf et al., 2020) and the Late Bronze Age (LBA) or Minoan eruption, the deposits of which are apparent in the present-day caldera cliffs, are characterised by a similar pyroclastic succession consisting of four major eruptive phases.

The precise date of the Minoan eruption, which is of paramount importance for the Late Bronze Age chronology, has been debated for almost a century (cf., Manning, 2014; Manning et al., 2020), when Marinatos (1939) put forward the idea, still popular in the public, that the decline of the Minoan culture in Crete sometime during the 15th

century BCE might have been due to the effects of the cataclysmic volcanic eruption, and in particular, an accompanying tsunami. However, Minoan tsunami deposits were verified only in the northeastern part of Crete (e.g., Dominey-Howes, 2004; Bruins et al., 2008), and today most scientists believe that even if the eruption may have weakened the Minoan civilisation, its ultimate decline occurred several decades if not a century later, due to internal societal conflicts, economic reasons, invasion by the Mycenaean Greeks, or even climatic changes (cf., Rehak and Younger, 1998; Tsonis et al., 2010; Dumas et al., 2015). Moreover, there is also a controversy with respect to the timing of the eruption between a 'low' (young) and 'high' (old) Egyptian chronology, which itself makes any relationship between the eruption and the fall of the Minoan civilisation problematic. Whereas archaeological synchronisms between Egypt, the Aegean and the Levant suggest an eruption date in the mid-15th century BCE (e.g., Warren et al., 2006; Wiener, 2009; Bronk Ramsey et al., 2010; Höflmayer, 2012), radiocarbon dating (on archaeological samples, buried wood, tree rings or speleothems) supports a 100–150 year older date, i.e. around 1630–1600 BCE (e.g. Friedrich

et al., 2006; Vinther et al., 2006; Siklósy et al., 2009; Badertscher et al., 2014; Manning, 2014; Demény et al., 2019; McAneney and Baillie, 2019). Recently, a detailed analysis of annual ring chronology of trees that lived at the time of the eruption revealed issues in the precision of radiocarbon calendar years, and yielded a younger eruption age between 1600 and 1525 BCE (Pearson et al., 2018; Kutschera, 2020) which overlaps with the date range from the archaeological evidence.

While the exact year and the direct effect on the Minoan civilisation in Crete is debated, it is no question that the eruption was a short-lived event (Druitt et al., 2019) that destroyed and completely covered with thick tuffs the archaeological site of Akrotiri located on the southern seashore of Santorini, which was excavated after its discovery by Marinatos in 1967. The main eruptive events were recently summarised by Druitt et al. (2019), building mainly on the work of Bond and Sparks (1976), Watkins et al. (1978), Heiken and McCoy (1990), Sigurdsson et al. (1990), Druitt et al. (1999), Druitt (2014), Johnston et al. (2014) and Nomikou et al. (2016). Here, we give an overview of the eruption phases (the deposits of which are denoted as units A to D by Druitt et al., 1999) focusing on the changes in pre-existing topography.

The Minoan eruption was preceded by earthquakes and, eventually, precursory explosions which left a few cm-thick ash-fall deposit on Santorini (Heiken and McCoy, 1990; Cioni et al., 2000). Although the timing of these events is not fully constrained, they might have allowed the inhabitants of Akrotiri to escape (Evans and McCoy, 2020), as no dead bodies were found (except one at Thirasia: Fouqué, 1879).

The first main phase of the Minoan eruption was a Plinian pumice fall which produced a deposit (unit A) up to 6 m thick (Bond and Sparks, 1976; Heiken and McCoy, 1984; Fig. 3). Based on isopachs (Bond and Sparks, 1976; Druitt et al., 1999; Cioni et al., 2000), the

vent of both the precursory and the Plinian phases was to the south of a pre-existing caldera (see below), which was located in the northern part of the present-day caldera. The caldera was occupied by an intracaldera island similar to the Kameni islands, referred to as 'Pre-Kameni' (Eriksen et al., 1990; Druitt and Francaviglia, 1992; Karátson et al., 2018b).

During the second phase, the vent migrated to the flooded caldera bay – in the vicinity of Pre-Kameni –, thus the eruption became phreatomagmatic (Druitt, 2014), resulting in up to 10-m-thick pyroclastic surge deposits (unit B). Thickest at the present-day caldera cliffs, these are interbedded with pumice-fall layers that originated from the still ongoing Plinian phase (Bond and Sparks, 1976; Druitt et al., 1999).

During the third phase, which remained phreatomagmatic, continuous eruption column collapse produced up to 55-m-thick, low-temperature (McClelland and Thomas, 1990) pyroclastic-flow deposits (unit C), again thickest near vent and thinning out distally (Bond and Sparks, 1976; Druitt et al., 1999). During this stage of the Minoan eruption, the pre-existing island of Strongyli, along with Pre-Kameni, started to get destroyed by the explosions, since a significant amount of different lithic clasts and also pumice clasts from previous eruptions are distributed in the deposits, in most places homogeneously (Druitt et al., 1999; Pfeiffer, 2001; Druitt, 2014), (Fig. 4). The largest, glassy andesite blocks (up to 10 m in size) were derived mostly from the destroyed Pre-Kameni island, and isopleths of the maximum clast size (≥ 3 m in diameter) indicate a vent still in the northern part of the caldera (Pfeiffer, 2001). Since the products of the first three phases were accumulated largely in the caldera, an intracaldera tuff construct or tuff cone (Johnston et al., 2014) may have formed, possibly until a complete caldera infill, and eventually blocking the access to sea water.

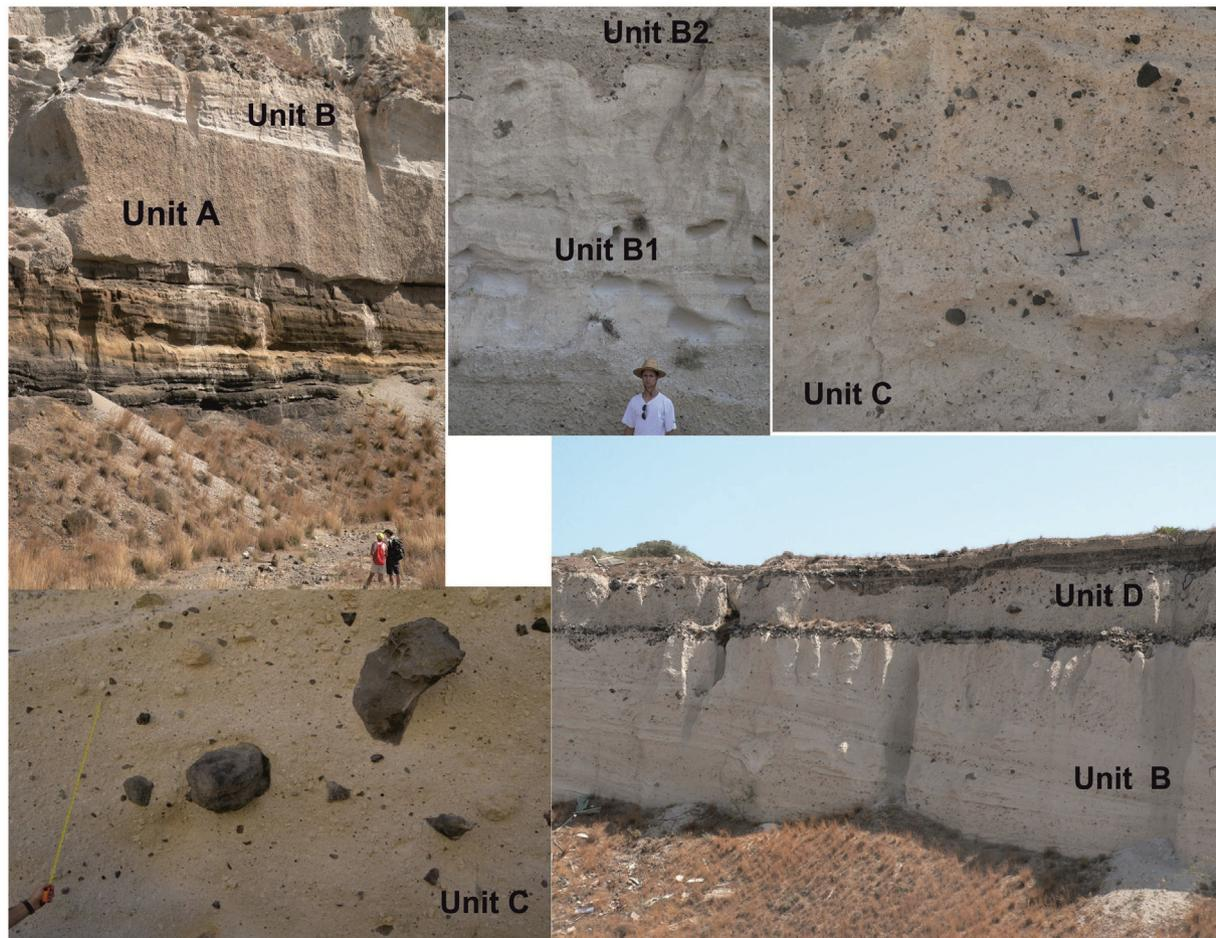


Fig. 3. Main units (A–D) of the Minoan eruption as exposed in the Fira and Mavromatis quarries at Thira; see text for details.

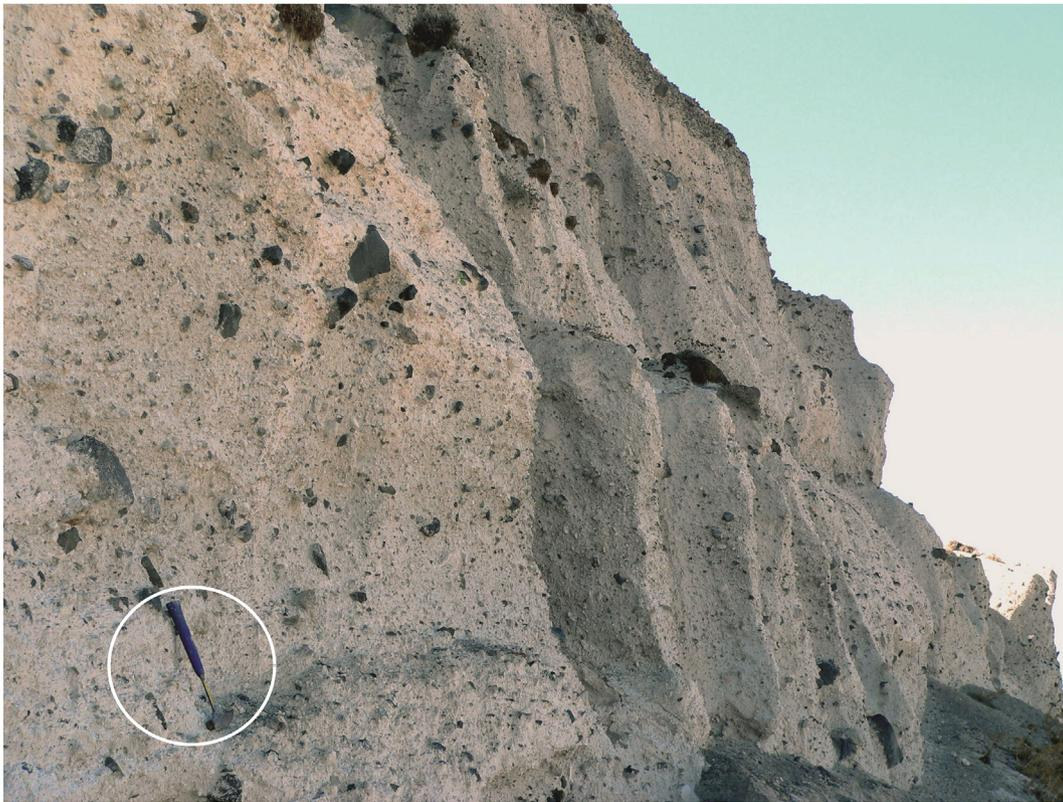


Fig. 4. Unit C is a low-temperature pyroclastic-flow deposit, showing randomly distributed clasts, the most striking of which are black glassy andesites up to a few m in diameter (Fira quarry, Thíra). Hammer for scale.

In the fourth phase, as a result of the shift from phreatomagmatic back to magmatic activity, higher temperature pyroclastic flows (McClelland and Thomas, 1990) were generated, resulting in the deposition of several tens of m-thick ignimbrites (unit D). On land, they form three fans (Druitt, 2014) in the N (Thirasia-Thíra), E and SE (Thíra), which may have been deposited successively on the basis of different lithic components, and which show distal thickening (Bond and Sparks, 1976), implying accumulation mostly in offshore settings (Sigurdsson et al., 2006). During this phase, the pyroclastic material may have been erupted from multiple vents (Druitt, 2014; Nomikou et al., 2016), and the opening of the subsequent vents was likely associated with gradual collapse of the new (i.e. present-day) caldera (Druitt, 2014).

The ignimbrites of the fourth phase are almost as rich in lithic clasts as unit C, in particular in the area of the N fan (Druitt, 2014). However, the lithic content is differently distributed; most of the lithics occur in horizons and lenses, and between lithic-poor and lithic-rich ignimbrite flow units there are also breccia units, showing various spatial relationships and depositional features implying both primary and secondary origin through reworking (Bond and Sparks, 1976; Druitt, 2014).

All units of the Minoan eruption contain juvenile components from the newly erupted magma and lithic clasts derived from older parts of Strongyli (Fig. 5; Heiken and McCoy, 1984; Druitt et al., 1999; Druitt, 2014; Karátson et al., 2018b). Following Druitt (2014), the latter can be grouped into black glassy andesite (BGA), flow-banded rhyolite, and miscellaneous lavas and tuffs. The lithics range in composition from basalt to rhyolite (50–71 wt% SiO₂), and principally have low Ba/Zr ratios that distinguishes them from a characteristic high-Ba/Zr group of clasts (mainly andesite) which is related to a new magmatic source (Druitt, 2014) subsequent to the previous Cape Riva Plinian eruption (21.8 ± 0.4 ka; Fabbro et al., 2013). Although some older (i.e. ≥530ka) high-Ba/Zr clasts also occur in the Minoan tuffs, BGA is the dominant lithology that constituted the Pre-Kameni island, in addition

to a smaller amount (up to a few vol%) of flow-banded rhyolite (Druitt, 2014; Karátson et al., 2018b).

High-precision, unspiked K-Ar dating of a single BGA sample was performed in the GEOPS laboratory (Orsay, France). Five independent analyses of the sample yielded ages ranging between 18.7 ± 3.1 and 21.5 ± 2.0 ka, resulting in a weighted mean age of 20.2 ± 1.0 ka (Karátson et al., 2018b). This can be considered as a minimum age for Pre-Kameni which may have begun construction soon after the Cape Riva eruption and have been active for many thousands of years.

3. Constraining the volume of the destroyed parts of Strongyli and Pre-Kameni on the basis of the lithic clast content

In order to reconstruct the Pre-Minoan landscape in a quantitative way, a precise volumetry of the Minoan tuffs as a whole and that of the pre-eruptive components (i.e. specific lithic clasts) is required. For instance, once the total volume is known, applying a photo-statistical analysis (at outcrop scale) can give numerical constraints on the proportion of various lithic clasts (Karátson et al., 2018a, 2018b), which can be linked to pre-existing parts of Strongyli destroyed during the Minoan eruption and used for topographic reconstruction. Certainly, the conclusions that can be drawn this way highly depend on volumetric constraints on the erupted material from geophysical or drilling data, either in intracaldera settings (Sakellariou et al., 2012; Johnston et al., 2014, 2015) or offshore (Sigurdsson et al., 2006; Hooft et al., 2019). Application of these methods should continue to get a full picture on the volumetry of the Minoan eruption. In this section, we summarize previous studies on volume estimates as well as our photo-statistical and granulometric approach (Karátson et al., 2018b).

On the basis of drill-core data from abyssal settings, Watkins et al. (1978) estimated ~13 km³ erupted magma (dense rock equivalent, DRE). Pyle (1990), using isopach and isopleth data in more detail, suggested a twofold volume of ~30 km³ DRE. This figure, without

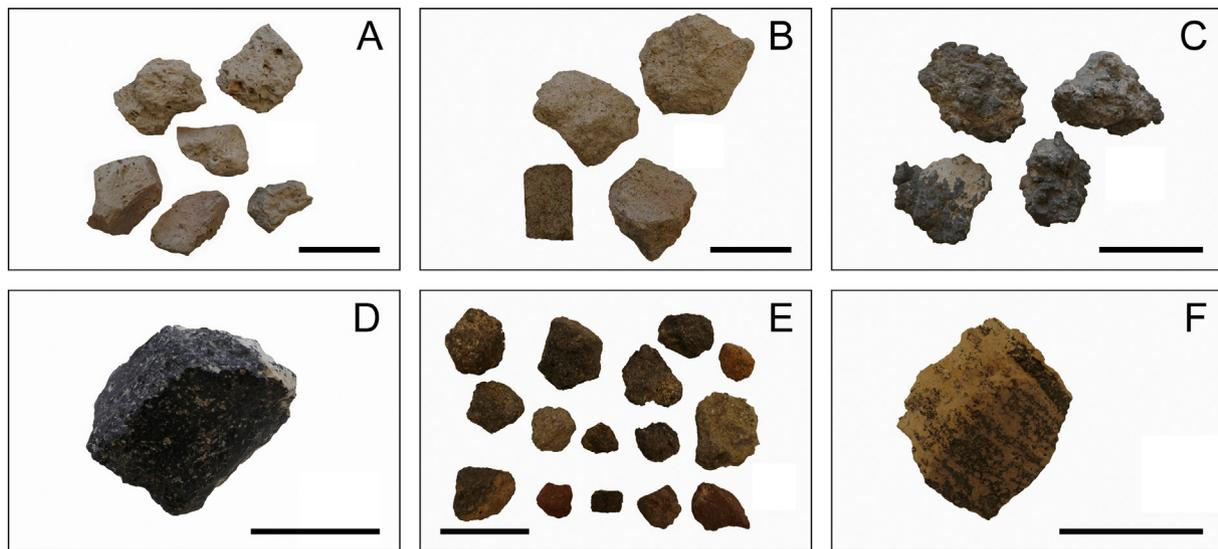


Fig. 5. Major juvenile (A–C) and lithic (D–F) clast types in the Minoan tuffs: (A) white, rhyodacitic pumice, (B) crystal-rich pumice, (C) andesitic blebs, (d) black glassy andesite (BGA), (E) miscellaneous lavas and tuffs, (F) flow-banded rhyolite. Scale bars are 5 cm long.

presenting details, was further doubled (60 km³) by Sigurdsson et al. (2006) referring to seismic profiles in offshore settings, and finally increased to 78–86 km³ by Johnston et al. (2014) who added significant caldera infill using seismic data and bathymetry. The latter volume, which should be considered a maximum estimate, corresponds to 117–129 km³ bulk (tephra) volume and increases the size of the Minoan eruption to VEI = 7, among the largest eruptions in the Holocene (Croswell et al., 2012; Johnston et al., 2014; Newhall et al., 2018).

Few studies have focused so far on the volume of lithic clasts contained in the Minoan tuffs. Pyle (1990) suggested 5–7 km³ in total, of which ~3 km³ represents the volume of Pre-Kameni (Druitt and Francaviglia, 1992). These figures have remained tentative in the subsequent literature without using a quantitative approach (e.g., Johnston et al., 2014).

In our previous study (Karátson et al., 2018b), applying a photo-statistical method and adopting the lithological discrimination of Druitt (2014), we addressed the total volume of the Minoan eruption and, within that, the volume of undifferentiated lithic clasts and those interpreted to have been derived from Pre-Kameni.

The concept of photo-statistics is the Delesse principle (Baddeley and Jensen, 2002); the proportion of total clast area (on adjusted, analysed photos) can be equal to the volumetric proportion of all (undifferentiated) lithic clasts under appropriate conditions. By taking representative photos, almost 80 sites were selected for statistical analysis (Karátson et al., 2018b); in addition to units A and B, the study mostly focused on unit C (which contains most of the clasts, evenly distributed), and unit D (selected outcrops included both lithic-poor ignimbrites and those containing lithic concentration horizons). Cumulative area of measured clasts (expressed in percentage of the total area of photo images) against the cumulative clast number shows a very strong logarithmic correlation, attributed to the rule that fragmentation of clasts during explosive eruptions follows a Weibull distribution (Fig. 6; cf., Wohletz and Brown, 1995). This means that smaller grains have a progressively smaller contribution to volume, but since the method is limited to <0.125 mm in the applied photo-analysis, the areal and hence volumetric proportion of the fine fractions should be determined using granulometry. Granulometric analysis performed on four samples, one from each unit, showed that the particles below 0.125 mm represent an important addition of ~40 wt% of the bulk material in the case of all units except unit A (where particles <0.125 mm account only for 6.5% of the total particles; Karátson et al., 2018b).

Results of the photo-statistics (Table 1), i.e. the average percentage of lithic clasts (of ≥ 0.125 mm) yielded 15.7 vol% in unit C, 13.8 vol% in unit D and, as expected, small values in unit A and B (1.8 and 0.8 vol%, respectively; Karátson et al., 2018b). In addition, granulometry of the <0.125 mm fraction showed that up to 10% vol% is represented by lithic clasts (Karátson et al., 2018b). Since the lithics correspond to various parts of the Minoan Strongyli island (Druitt, 2014), these figures unambiguously confirm that the destruction of Strongyli, including Pre-Kameni, occurred mostly during the climactic phases (3 and 4) of the Minoan eruption. However, we note that the obtained high percentage of lithics in unit D, in addition to the occurrence of clasts from block-rich pyroclastic flows (Druitt, 2014), may be partly due to an unconstrained amount of reworked lithic content.

To attach bulk volumetric values to the obtained lithic clast proportion values, we considered the total maximum volume of the Minoan tuffs of 123 km³ (i.e. the mean of 117–129 km³ of Johnston et al., 2014) and distinguished between the four main units (Karátson et al., 2018b). As for the intracaldera pyroclastic-flow deposits, we proportioned the intracaldera volumes (36 km³, mean of 31–41 km³ of Johnston et al., 2014) between A, B and C according to isopach data from the literature (Karátson et al., 2018b). A main issue was how to

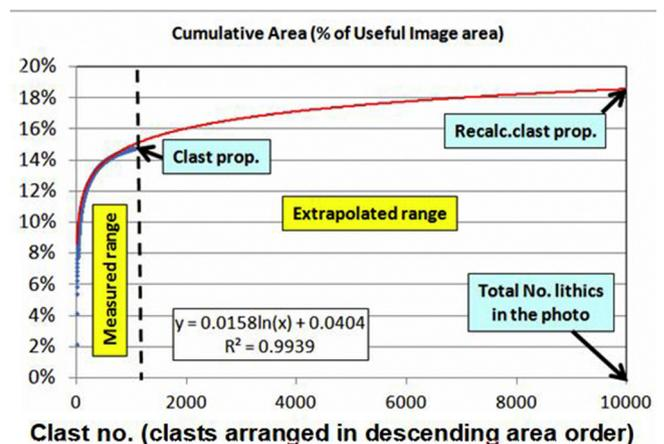


Fig. 6. Example of photo-statistics (Fira quarry, Thira): cumulative area (%) of lithic clasts (within analysed image) versus number of lithics (arranged in decreasing size). Modified from Vereb (2016), Karátson et al. (2018b).

Table 1

Unit	Volume (km ³)	Lithic clast vol% from photo-statistics		of which black glassy andesite vol%		Volume of total lithic content (km ³)		Volume of 'Pre-Kameni' (km ³)	
A	37.6	1.8 ± 0.6		3.8 ± 0.9		0.67 ± 0.28		0.03 ± 0.01	
B	7.8	0.8 ± 0.2		16.8 ± 2.8		0.06 ± 0.02		0.01 ± 0.00	
C	25.9	15.5	15.7 ± 1.2	30.4 ± 3.1	4.06 ± 0.52	2.43 ± 0.31	1.23 ± 0.16	0.74 ± 0.09	
D	51.7	62.1	13.8 ± 5.7	10.8 ± 1.0	7.14 ± 3.00	8.57 ± 3.61	0.77 ± 0.33	0.93 ± 0.39	
Sum	123				11.93 ± 3.82	11.74 ± 4.22	2.04 ± 0.50	1.70 ± 0.50	
Additional lithics ¹	123*40%=49.2		10	10		4.92		0.492	
Total	123				16.85 ± 3.82	16.66 ± 4.20	2.53 ± 0.50	2.19 ± 0.50	

Maximum volume estimates (Johnston et al., 2014) of the Minoan eruptive units (A–D; for A, including co-ignimbrite ash), their lithic content, and within the latter, the contribution of the black, glassy andesite (i.e. 'Pre-Kameni' island) using data from literature, photo-statistics, and granulometry (Karátson et al., 2018b and references therein). Values are given in one decimal for volume, two decimals for lithic content. In the first and the last two columns, left panels show values assuming that the ratio of unit C:D is 1:2; right panels show values assuming that the ratio of unit C:D is 1:4 (see text). ¹Additional lithics from the finest (<0.125 mm) fraction of all units resulting from sieving. Of the total lithic content, the volume of Pre-Kameni is considered as consisting exclusively of the black glassy andesite, i.e. without the volumetrically minor flow-banded rhyolite. The difference of the volumes of the total lithics and Pre-Kameni gives the destroyed part ($14.4 \pm 0.8 \text{ km}^3$) of the Minoan ring island of Strongyli.

divide the bulk volume of units C and D, since, as mentioned above, most of the latter is found in submarine settings where no data exist about their proportion. We considered two possibilities: a ratio of unit C:D of 1:2 or 1:4 (the latter is arguably more realistic, if we assume large volumes of unit D distally; Karátson et al., 2018b).

In order to constrain the volume of Pre-Kameni island, starting from the proportioned maximum bulk (tephra) volumes, we calculated the total lithic content and, within that, the volume of BGA clasts (Karátson et al., 2018b; Table 1). As mentioned above, the volume of BGA clasts corresponds to the overwhelming majority of the volume of Pre-Kameni (apart from a few % of flow-banded rhyolite lava clasts). The volume of total lithics is 16.9 ± 3.8 or $16.7 \pm 4.2 \text{ km}^3$, and the volume of BGA clasts (i.e. Pre-Kameni) is 2.5 ± 0.5 or $2.2 \pm 0.5 \text{ km}^3$, the first and second figures corresponding to ratios of C:D = 1:2 and 1:4, respectively. As seen from the obtained values, even if the unconstrained proportion between unit C vs D in submarine settings results in some uncertainty, it does not significantly alter the main results on lithic clast volumes.

However, there are at least two more issues that introduce further uncertainties in addition to that the calculation took account the maximum tephra volume. First, our photo-statistical findings were based on on-land outcrops without any information on the correlative submarine deposits, although it is known that the percentage of lithic components in ignimbrites commonly decreases with increasing distance from source (e.g., Druitt and Bacon, 1986). Therefore, the obtained lithic content of the Minoan ignimbrite, based on proximal samples, is probably a maximum estimate. By contrast, certain volumes of Strongyli (and Pre-Kameni) may have been sunken during caldera formation, not represented in the Minoan tuffs, which may increase the real total volumes. These questions can only be clarified reliably via drillings and seismic studies both in the caldera and offshore Santorini. We address these questions using a topographic reconstruction approach in the Discussion.

4. Evolution of the interpretation of the Late Bronze Age landscape

Before discussing the available data related to the Late Bronze Age topography, it is important to know how landscape reconstruction has evolved (Fig. 7). This problem has a long history, inspired first by the "round shape" of Strongyli, which suggested an intact, circular island for many early researchers (e.g., Fouqué, 1879), possibly with a central cone as high as 500–800 m (Pichler and Kussmaul, 1972; Bond and Sparks, 1976).

It was first Heiken and McCoy (1984) who contradicted this idea and proposed the existence of a caldera prior to the Minoan eruption in the south of the present-day caldera. By contrast, Druitt et al. (1999) showed from mapping that, had this caldera existed, it had already been filled up with tuffs long before the Minoan eruption.

Subsequently, three lines of evidence emerged confirming a pre-existing caldera prior to the Minoan eruption. Friedrich et al. (1988) and Eriksen et al. (1990), later completed by Anadón et al. (2013), reported the presence of stromatolites and travertines in the Minoan tuffs (in the N part of Thíra and Thirasia) as direct evidence of a shallow, pre-existing flooded caldera. Druitt and Francaviglia (1992) pointed out patches of in situ Minoan pumice adhering to the modern NE caldera, which proved that those cliffs existed prior to the Minoan eruption. More recently, the formation of the northern walls of the present-day caldera was determined by ³⁶Cl exposure dating, verifying that the inward-looking cliffs of both Thirasia and N Thíra already existed in the Late Bronze Age (Athanasas et al., 2016).

Accordingly, as a recent overview (Druitt et al., 2019) summarised, there is consensus now that the pre-Minoan caldera was a flooded bay restricted to the northern part of the present-day caldera (Fig. 7). By contrast, the existence of an opening is debated; earlier work commonly preferred a western entrance (e.g., Friedrich et al., 1988), whereas more recent findings favour a narrow opening, if any, to the north (e.g., Athanasas et al., 2016; Nomikou et al., 2016). Importantly, Nomikou et al. (2016) pointed out that the present-day outlet channel between Thíra (Oia) and Thirasia was created as the sea broke into the newly formed caldera, whereas two more openings between Thirasia-Aspronisi and Aspronisi-Thíra were generated subsequently.

5. Discussion

5.1. The pre-existing caldera as shown by archaeological evidence

The archaeological site of Akrotiri has been the intense focus of various interests for over half a century. Like Pompeii (Kockel and Schütze, 2016), it preserved a large number of wall paintings that are unparalleled for its particular culture. As the chronological debate of the eruption continues, art historians scrutinize the treasure trove of Bronze Age frescoes, but often overlook the volcanological discovery of the flooded caldera in Minoan times, as outlined above.

The presumption that Strongyli once formed a central volcanic cone had implications for the interpretation of the so-called Flotilla Fresco, which is one of the well-preserved wall paintings from the West House at the Akrotiri site. The landmasses and cities on the fresco's sides were interpreted to represent departure and arrival points for the fleet (Marinatos, 1967–1974). With an inundated caldera at Strongyli, we can understand the landmasses to represent the capes that bordered the single entrance into the caldera (Fig. 8). They do not have to represent locations of departure and arrival that are distantly separate.

From the very beginning, the Flotilla Fresco was thought to represent a voyage from Libya to Strongyli, although the points of origin were debated (Marinatos, 1967–1974; Dumas, 1992; Strasser, 2010). On the wall opposite from the Flotilla Fresco, the Shipwreck Fresco

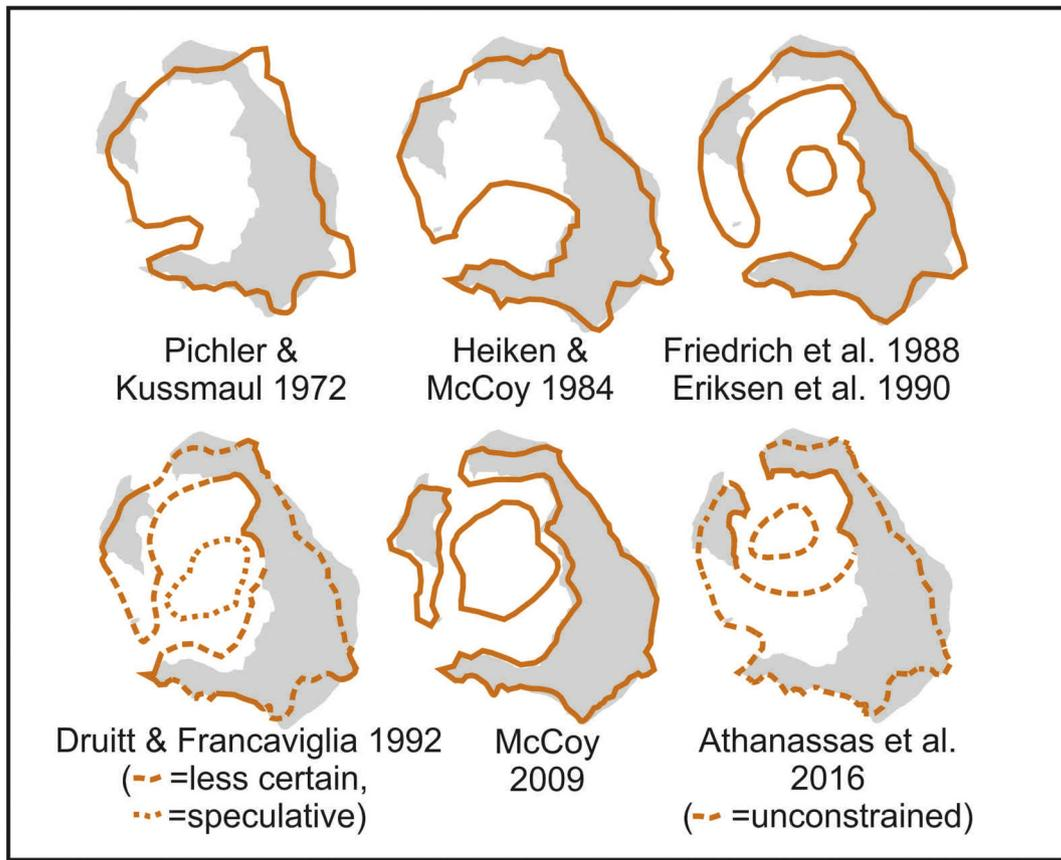


Fig. 7. Evolution of interpretation of the Late Bronze Age landscape of Santorini (modified from Karátson et al., 2018b).

served as basis for the interpretation of a militaristic “Libyan Expedition” (Marinatos, 1967-1974) because it contains African elements. Despite volcanological data demonstrating that an inundated caldera

existed at Strongyli prior to the Minoan eruption, the art historical interpretation of the Flotilla Fresco portraying a voyage solidified (e.g., Wayland-Barber and Barber, 2006). In other words, while the

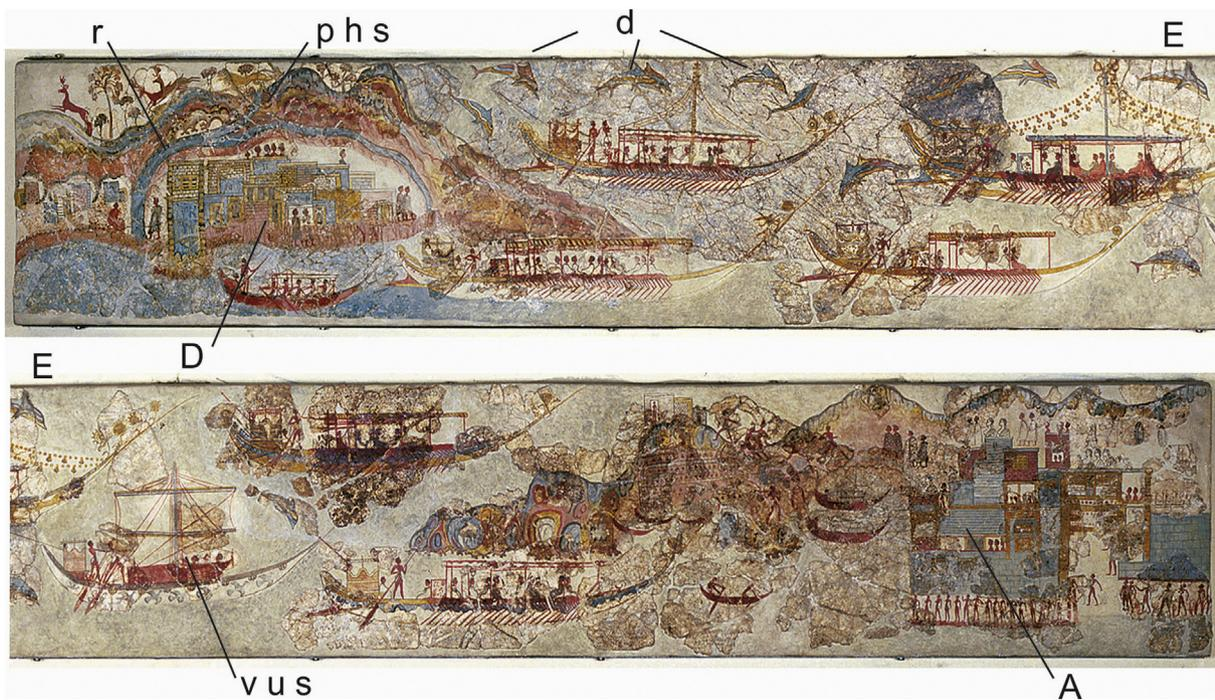


Fig. 8. The Flotilla Fresco (cropped into two parts; upper part is the left side of the fresco) from the south wall of Room 5 in the West House at Akrotiri. Abbreviations: r - rivers, D = Departure Town, p h s = parallel, horizontal stratigraphy of internal caldera cliffs, d - dolphins, E = entrance (opening), v u s = vessel with unfurled sail, A = Arrival Town. (Reproduced courtesy of the Thera Foundation; Strasser, 2010).

specifics of the Flotilla Fresco were debated, the general concept of a voyage from somewhere to a solid, cone-shaped Strongyli was the premise. More recently, [Strasser \(2010\)](#) proposed that the Flotilla Fresco is a realistic landscape of the Strongyli caldera, possibly as viewed towards the northwest ([Fig. 9](#)), and this in turn solves many iconographical problems that the “voyage” interpretation cannot ([Strasser and Chapin, 2014](#)):

- 1) Only one vessel has its sail unfurled, while paddlers propel all the others, militating against the idea of a long distant voyage;
- 2) The depiction of a landscape explains why some boats and dolphins are positioned above the land rather than in the sea. A basic concept used by ancient artists is the cartographic perspective, whereby objects behind are placed above and those in front are positioned below. This convention was quite common in contemporary Egyptian art. In this case, the perspective is from the southeast, so the boats and some dolphins are shown both above and below the two landmasses, because some are inside the caldera, and others outside;
- 3) The horizontal depiction of rocks around Town 2 (also known as Departure Town) on the left side of the fresco is rare. The Aegean Bronze Age convention for rocks in frescoes was usually in vertical registers ([Strasser, 2010](#)). Moreover, the horizontal depictions of rocks, possibly as layers, might represent a quasi-realistic stratigraphy exposed in the interior of the caldera. The blue stripes around the Departure Town are typical in Aegean paintings to represent rivers. The other blue areas may simply be grass, since the colour green is almost unknown in Aegean paintings. The reddish colour in turn may represent scoriaceous units, which are widespread around present-day Oia for instance;
- 4) The large boats are festooned for a celebration of some sort, which indicates that they were decorated for observations by people nearby, and therefore the vessels are not out at sea. Paddling (not rowing), a less efficient means of propulsion, might be part and parcel of the event's ceremonial nature ([Wachsmann, 1998](#)).

One might postulate that “flotilla” frescoes are a genre in the Aegean Bronze Age as similar examples have been found at Ayia Irini (Kea)

([Morris, 1989, 2000](#)), at Pylos ([Brecoulaki et al., 2015](#)) and at Iklaina ([Cosmopoulos, 2015](#)). This does not, however, preclude the idea that a specific location is also represented.

It is important to keep in mind that Akrotiri is not a palace, such as those found on Crete, where one might expect propagandistic art as a narrative. Even then, we do not find such military propaganda, which is one of the surprising characteristics of Minoan art ([Doumas, 1992](#)). These are paintings that adorn the West House with animals held on the first floor and a bathroom on the second, and might be simply decorative, with little combining iconography or thematic scheme. Although the maritime theme is apparent in most of the West House paintings, there is still an exception in the “Young Priestess” Fresco ([Doumas, 1992](#)). Consequently, all the West House frescoes do not necessarily follow a narrative.

In addition, there is no reason to unite all three miniature frescoes of Room 5 in the West House ([Warren, 1979](#)). They have no iconographical elements in common to connect them ([Doumas, 1992](#)) and, indeed, the frescoes are of different heights due to the cross beams on the ceiling ([Palyvou, 2005](#)). Thus, if we view the Flotilla Fresco in isolation, accepting the interpretation of [Strasser \(2010\)](#) and [Strasser and Chapin \(2014\)](#), we can recognise a valid presentation of Strongyli's landscape prior to the Minoan eruption.

However, if the fresco is a quasi-realistic landscape, the apparent hummocky terrain above both at the Departure and Arrival towns as well as the location of the towns at the foot of steep caldera walls require an explanation. In this respect, even if the Cape Riva caldera could have been a smaller depression with less pronounced caldera cliffs, the morphology in the northern part of Thirasia and Thira comprising pre-Cape Riva formations should have been similar to the present caldera with steep, hummocky terrain. Second, and more importantly, at least fifteen Late Bronze Age sites have been confirmed on Santorini, several of which facing the interior of the caldera (e.g., [Wagstaff, 1978](#); [Hope Simpson and Dickinson, 1979](#); [Aston and Hardy, 1990](#); [Doumas, 1992](#); [Friedrich, 2000](#)). Moreover, as presented by [Aston and Hardy \(1990\)](#), the height of the caldera cliffs might have been lower and some of the inward slopes less steep than today ([Vassilopoulos et al., 2009](#); [Antoniou et al., 2017](#)) because the seashore level was higher prior to the 300–400 m deep Minoan caldera collapse.

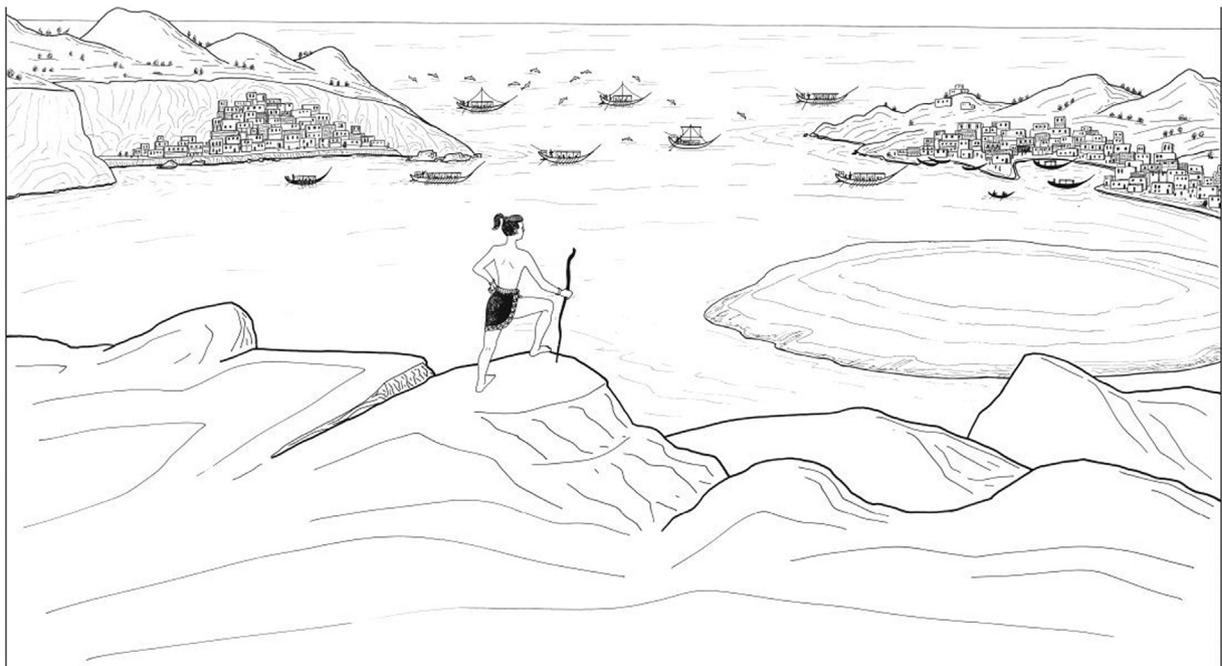


Fig. 9. Reconstruction of the perspective of the Flotilla Fresco depicting a landscape prior to the Late Bronze Age eruption, looking possibly towards the northwest (drawing by D. Faulmann; [Strasser, 2010](#)).

Finally, Late Bronze Age sites facing from the northern caldera bay include sites found in the quarries at Oia (northwest Thíra) and Manolas (Thirasia), which, assuming a northwest entrance in between, may be tentatively related to the Departure and Arrival towns, respectively. In this respect, findings by Athanassas et al. (2016) do not allow a western entrance, south of present-day Thirasia, as the southern cliffs of Thirasia were formed during the Minoan eruption.

5.2. Towards reconstructing the topography of Strongyli prior to the Minoan eruption

The volume of lithic clasts in the Minoan tuffs (Karátson et al., 2018b) makes it possible to constrain the volume, and therefore to reconstruct a possible topography, of Strongyli prior to the Minoan eruption. Our concept is that the obtained volume of the lithic content, corrected by taking into account the minimum and maximum volume estimates of the erupted material, can be added to the recent topography, and visualized by using a digital elevation model (DEM) approach.

The main steps of creating a reconstructed DEM (expanding on Karátson et al., 2018b) are as follows. We delineated an area in the SW where we intended to replace the present-day topography (see Fig. 1C) with the reconstructed one. The N part of the boundary of the pre-Minoan (Cape Riva) caldera remained the same as today (cf., Athanassas et al., 2016), even though minor topographic changes such as landslides might have occurred along the cliffs during the eruption. The W and SW parts of the caldera boundary were aligned with the actual W part of the caldera rim line which today is slightly below the sea level near Aspronisi. In the S and E, the caldera boundary line was drawn along the present-day caldera rim. The elevation of the vertices of the

boundary line was corrected to the actual DEM elevation. Then, the arcuate line of the former caldera rim was drawn between the W and E endpoints. All subsequent contour lines were manually created between the former caldera rim and the former sea level at equal intervals. The endpoints at the reconstruction area boundary were adjusted to the present-day contour lines. To create a new DEM, we took into consideration these contour lines and the reconstruction area boundary, and used the natural neighbour interpolation between the contours. When calculating the volume of added terrain (i.e. the difference between any reconstructed DEM and the present-day DEM), we used the reconstructed DEM as the upper surface and the present-day DEM as the lower surface and applied the 'volume calculation tool' of the Golden Software Surfer.

In order to make the smooth surface of the new DEM more realistic, we increased the small-scale surface roughness of the present slopes by generating a weakly developed random drainage network with gullies incised into the surface by less than ten metres (according to their Strahler stream order; Strahler, 1957). These small streams are negligible in terms of volumes.

Using the above considerations on the pre-eruptive topography, several solutions are possible under the assumption that the northern depression existed already whereas the southern depression formed during the Minoan eruption. In Fig. 10, two alternative options are presented in newly constructed DEMs, showing a larger flooded caldera (with a lower caldera rim 200 m asl) in Fig. 10A, and a smaller flooded caldera (with a higher caldera rim 260 m asl) in Fig. 10B. Both reconstructions are based on our previous calculations of 16.9 km³ maximum total lithic content (Karátson et al., 2018b) and the existence of pre-Minoan Cape Riva caldera cliffs as evidenced by Athanassas et al.

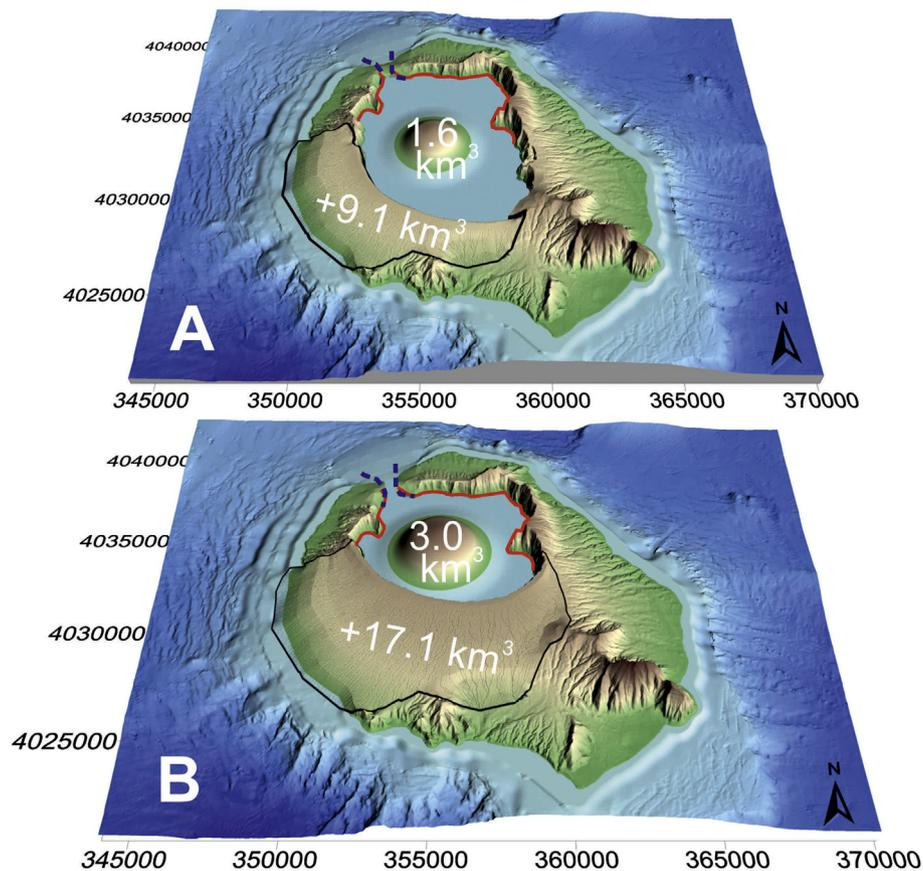


Fig. 10. Two contrasting alternatives of reconstructing the topography of Pre-Minoan Santorini ('Strongyli') on DEM image. UTM coordinates are shown on both axes. Pre-existing caldera cliffs (cf., Athanassas et al., 2016) are marked in red, added volumes in black line, respectively. Note that pre-existing (northern) caldera cliffs may have been slightly different from present topography. See text for discussion.

(2016). However, they take into account the total erupted (bulk) volume of the Minoan tuffs and the destroyed part of Strongyli differently. These two alternatives are explained and discussed as follows.

Fig. 10A shows the smallest possible volume of Strongyli (and within that, Pre-Kameni), implying a relatively large caldera. Numerically, this model considers the minimum volume estimate of 52 km³ DRE of the Minoan tuffs consisting of the 30 km³ estimate by Pyle (1990) plus the 22 km³ mean volume within the caldera (Johnston et al., 2014). Considering a 1.5 ratio of the erupted tephra (bulk) to DRE volume (i.e., 123 km³ mean bulk volume to 82 km³: Johnston et al., 2014), 52 km³ DRE corresponds to 78 km³ bulk. In a similar way, considering a 7.3 ratio of the erupted tephra to lithic volume (i.e., 123 km³ mean bulk volume to 16.9 km³ lithic volume), 78 km³ bulk volume would contain 10.7 km³ total lithics. Of the latter figure, using the proportions between BGA and total lithic content obtained by photo-statistics (Table 1), a volume of 1.6 km³ is interpreted to be derived from Pre-Kameni (BGA) assuming that the ratio of unit C:D is 1:2. These minimum volumes are presented and marked in Fig. 10A, where the pre-eruptive terrain of Strongyli is 9.1 km³, hosting a Pre-Kameni island of 1.6 km³ (=10.7 km³ altogether). However, this scenario is considered less realistic, as the caldera cliffs extends significantly to the south well beyond the outlines pointed out by Athanassas et al. (2016), and is therefore inconsistent with the finding that the Late Bronze Age caldera was restricted to a northern basin (see above).

By contrast, Fig. 10B leaves unaffected the outline of those cliffs that indisputably existed before the Minoan eruption (Athanassas et al., 2016), and reconstructs the pre-eruptive terrain of Strongyli with the largest possible extent. This time, with no consideration of the obtained 16.9 km³ total lithic content, the caldera rim is drawn as a regular circle encompassing the smallest possible pre-existing caldera. Such a reconstructed DEM results in an added terrain of 17.1 km³ to the ring island, i.e. 1.88 times more than in the previous approach (9.1 km³). Based on this proportion, the volume of Pre-Kameni is constrained to 3.0 km³.

Notably, the 17.1 km³ of added terrain — which again is the maximum spatially possible value — is only ~2.7 km³ larger than the value obtained for the ring-island of Strongyli by photo-statistics and granulometry (14.4 ± 0.08 km³; Table 1). We propose that the volume difference can be accounted for by assuming sunken (downfaulted) parts of Strongyli, which are therefore not incorporated in the Minoan

tuffs. In this scenario, Pre-Kameni, with its 3.0 km³ volume, still remains relatively small (corresponding approximately to the dimensions of present-day Palaea and Nea Kameni, whose combined volume is ~3.2 km³: Nomikou et al., 2014). Such a topographic reconstruction is considered a more realistic scenario based on the results of Druitt (2014) and Athanassas et al. (2016), and is in accordance with the maximum volume estimate of the Minoan tuffs.

A further issue which is difficult to assess in terms of palaeotopography is the relation between the collapsed volume and the depth of sea water in the flooded caldera. As discussed by Johnston et al. (2014, 2015), Nomikou et al. (2016) and Hooft et al. (2019), the Minoan tuffs, which accumulated in the caldera and were downfaulted in the fourth phase of the eruption, comprise a several hundred metre thick succession that is underlain by the sunken Pre-Minoan deposits at a depth of 1–5 km below the surface. The precise location and thickness of the latter, and their volumetric contribution to Late Bronze Age Strongyli, can only be constrained by seismic data and further drilling. However, for spatial reasons based on our DEM analysis, the addition to the ring island of the destroyed on-land volume of Strongyli, which might have been downfaulted in the present caldera, cannot be more than ~2.7 km³.

In terms of landscape evolution during the Minoan eruption (Fig. 11), the initial topography should have consisted of a shallow, small northern flooded caldera encompassed by the main ring island of Strongyli, depicted with a maximum possible volume in Fig. 11A. During the first three phases of the eruption, as proposed by Johnston et al. (2014), the presently observable elevated position of the Minoan tuffs on the caldera cliffs, along with the downfaulted masses in the caldera, argue for the creation of a tuff construct or tuff cone in the caldera. In this context, phases 1, 2 and 3 can be interpreted as eruptive periods during which the elevation of Strongyli was increased and the topography became conical (Fig. 11B). Phase 4 was, however, different in terms of tephra accumulation. The products deposited during this phase show significant facies variations (Bond and Sparks, 1976; Druitt, 2014), ranging from lithic poor, massive, tan ignimbrites to lag breccias and lithic block-rich ignimbrites as well as subordinate debris-flow deposits and fluvial gravel beds on top. These deposits preferably filled the topographic lows towards distal areas; therefore, as shown earlier, most of their volume accumulated offshore. Such a relief, indicated in Fig. 11C,

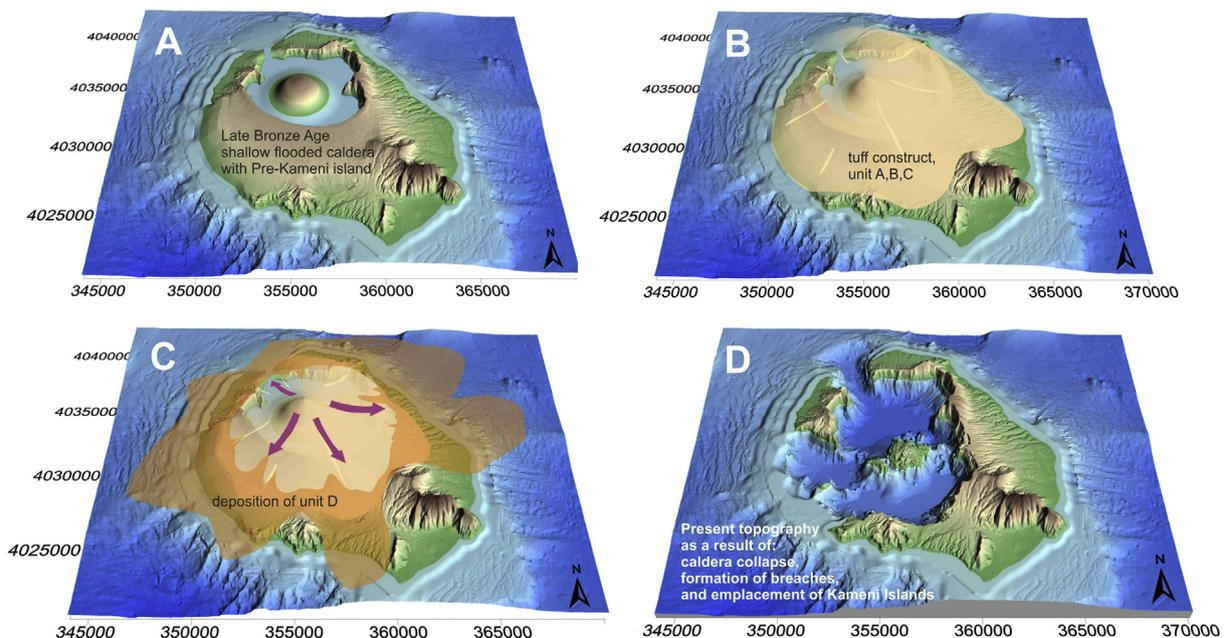


Fig. 11. Proposed landscape evolution of Strongyli during the Minoan eruption as represented in subsequent DEM images. (UTM coordinates are shown on both axes.)

might have existed for some time into phase 4 of the Minoan eruption, when it was truncated by caldera collapse (Bond and Sparks, 1976; Druitt, 2014) as depicted in Fig. 11D.

6. Conclusions

The extent and topography of the island of Santorini ('Strongyli') in the Late Bronze Age can be assessed by analysing the lithic content of the Minoan tuffs. Considering various alternatives for the total erupted (bulk) volume and the size of the flooded caldera, we discussed two end-member models of topographic reconstructions presented on DEM images. Both are in agreement with archaeological interpretation of the Flotilla Fresco which is suggested to depict a realistic landscape characterised by a relatively small flooded bay corresponding to a pre-existing caldera (formed during the 22 ka Cape Riva eruption), possibly open to the northwest.

The first model which is based on the minimum volume estimate of the Minoan tuffs (52 km³ DRE) shows a large pre-existing caldera. However, such a reconstructed topography does not fit with previous findings about a caldera restricted to the north (e.g. Druitt, 2014; Athanassas et al., 2016; Nomikou et al., 2016).

The second model starts from the largest DRE volume of 82 km³ of the Minoan tuffs, and adds the topographically possible maximum terrain to the ring island, leaving untouched rigorously only the pre-existing caldera cliffs (Athanassas et al., 2016). Such a maximum added terrain volume, ~17.1 km³, is ≤3 km³ larger than the volume obtained from the total lithic content of the Minoan tuffs (Karátson et al., 2018b), which can be accounted for by, for example, downfaulted (sunken) parts of Strongyli within the caldera.

Using the second model, DEM representation of subsequent phases of the Minoan eruption depicts a syn-eruptive, conical infill of tuffs in the central part of Strongyli, which was truncated by late-stage caldera collapse.

Declaration of competing interest

The authors declare no competing interests.

Acknowledgments

DK, TT and VV thank for the financial support from Hungarian National Grant NKFIH OTKA K115472, K131894 and an ELTE open access grant. RG acknowledges financial support from Keele University. Multi-beam data were obtained aboard R/V AEGAEON of HCMR during 2001 (in the framework of GEOWARN project IST-1999-12310) and 2006 (THERA 2006, OCE-0452478, supported by grant from the National Science Foundation). We thank the captain and crew of the R/V AEGAEON for their help and great skills in carrying out the exploration of Santorini Volcano. This is Laboratory of Excellence ClerVolc contribution number 409. Thanks go to two anonymous reviewers and editorial handling by Alessandro Aiuppa.

References

Anadón, P., Canet, C., Friedrich, W.L., 2013. Aragonite stromatolitic buildups from Santorini (Aegean Sea, Greece): geochemical and palaeontological constraints of the caldera palaeoenvironment prior to the Minoan eruption (ca 3600 yr bp). *Sedimentology* 60 (5), 1128–1155.

Antoniou, V., Lappas, S., Leoussis, C., Nomikou, P., 2017. Landslide risk assessment of the Santorini volcanic group. *GISTAM 2017 - Proceedings of the 3rd International Conference on Geographical Information Systems Theory, Applications and Management*, p. 131.

Aston, M.A., Hardy, C.G., 1990. The pre-Minoan landscape of Thera: a preliminary statement. In: Hardy, D.A., Dumas, C.G., Sakellaris, J.A., Warren, P.M. (Eds.), *Thera and the Aegean World*, III, 1, pp. 348–360.

Athanassas, C., Bourlès, D., Braucher, R., Druitt, T., Nomikou, P., Leanni, L., 2016. Evidence from cosmic ray exposure (CRE) dating for the existence of a pre-Minoan caldera on Santorini, Greece. *Bull. Volcanol.* 78 (5), 35.

Baddeley, A.J., Jensen, E.B.V., 2002. *Stereology: Sampling in Three Dimensions*. University of Western Australia. Department of Mathematics and Statistics.

Badertscher, S., Borsato, A., Frisia, S., Cheng, H., Edwards, R., Tüysüz, O., Fleitmann, D., 2014. Speleothems as sensitive recorders of volcanic eruptions—the Bronze Age Minoan eruption recorded in a stalagmite from Turkey. *Earth Planet. Sci. Lett.* 392, 58–66.

Bocchini, G., Brüstle, A., Becker, D., Meier, T., van Keken, P., Ruscic, M., Papadopoulos, G., Rische, M., Friederich, W., 2018. Tearing, segmentation, and backstepping of subduction in the Aegean: new insights from seismicity. *Tectonophysics* 734, 96–118.

Bond, A., Sparks, R., 1976. The Minoan eruption of Santorini, Greece. *J. Geol. Soc.* 132 (1), 1–16.

Brecoulaki, H., Stocker, S.R., Davis, J.L., Egan, E., 2015. An Unprecedented Naval Scene from Pylos: First Considerations. *Mycenaean Wall Paintings in Context: New Discoveries, Old Finds Reconsidered*. National Hellenic Research Foundation, Institute of Historical Research, Athens, pp. 260–291.

Bronk Ramsey, C., Dee, M.W., Rowland, J.M., Higham, T.F., Harris, S.A., Brock, F., Quiles, A., Wild, E.M., Marcus, E.S., Shortland, A.J., 2010. Radiocarbon-based chronology for dynastic Egypt. *Science* 328 (5985), 1554–1557.

Bruins, H.J., MacGillivray, J.A., Synolakis, C.E., Benjamins, C., Keller, J., Kisch, H.J., Klügel, A., Van Der Plicht, J., 2008. Geoarchaeological tsunami deposits at Palaiakastro (Crete) and the Late Minoan IA eruption of Santorini. *J. Archaeol. Sci.* 35 (1), 191–212.

Cioni, R., Gurioli, L., Sbrana, A., Vougioukalakis, G., 2000. Precursory phenomena and destructive events related to the Late Bronze Age Minoan (Thera, Greece) and AD 79 (Vesuvius, Italy) Plinian eruptions; inferences from the stratigraphy in the archaeological areas. *Geol. Soc. Lond. Spec. Publ.* 171 (1), 123–141.

Cosmopoulos, M., 2015. A Group of New Mycenaean Frescoes from Iklaina, Pylos. *Mycenaean Wall Painting in Context: New Discoveries, Old Finds Reconsidered*. National Hellenic Research Foundation, Institute of Historical Research, Athens, pp. 249–259.

Crowther, H.S., Arora, B., Brown, S.K., Cottrell, E., Deligne, N.L., Ortiz, N., Hobbs, L., et al., 2012. Global database on large magnitude explosive volcanic eruptions (LaMEVE). *J. Appl. Volcanol.* 1 (13 p).

Demény, A., Kern, Z., Czuppon, G., Németh, A., Schöll-Barna, G., Siklósy, Z., Leél-Össy, S., Cook, G., Serlegi, G., Bajnóczi, B., Sümegei, P., Király, Á., Kiss, V., Kulcsár, G., Bondár, M., 2019. Middle Bronze Age humidity and temperature variations, and societal changes in East-Central Europe. *Quat. Int.* 504, 80–95.

Dominey-Howes, D., 2004. A re-analysis of the Late Bronze Age eruption and tsunami of Santorini, Greece, and the implications for the volcano–tsunami hazard. *J. Volcanol. Geotherm. Res.* 130 (1–2), 107–132.

Doumas, C., 1992. *The Wall-paintings of Thera*. Thera Foundation.

Doumas, C.G., Palyvou, K., Devetzi, A., Boulotis, C., 2015. Akrotiri, Thera 17th Century BC: A Cosmopolitan Harbour Town 3,500 Years Ago. *Society for the Promotion of Studies on Prehistoric Thera* (99 p).

Druitt, T.H., 2014. New insights into the initiation and venting of the Bronze-Age eruption of Santorini (Greece), from component analysis. *Bull. Volcanol.* 76 (2), 794.

Druitt, T.H., Bacon, C.R., 1986. Lithic breccia and ignimbrite erupted during the collapse of Crater Lake caldera, Oregon. *J. Volcanol. Geotherm. Res.* 29, 1–32.

Druitt, T., Francaviglia, V., 1992. Caldera formation on Santorini and the physiography of the islands in the late Bronze Age. *Bull. Volcanol.* 54 (6), 484–493.

Druitt, T., Mellors, R., Pyle, D., Sparks, R., 1989. Explosive volcanism on Santorini, Greece. *Geol. Mag.* 126 (2), 95–126.

Druitt, T.H., Edwards, L., Mellors, R., Pyle, D., Sparks, R., Lanphere, M., Davies, M., Barreirio, B., 1999. Santorini volcano. *Geol. Soc. Mem.* 19.

Druitt, T., Mercier, M., Florentin, L., Delouie, E., Cluzel, N., Flaherty, T., Médard, E., Cadoux, A., 2016. Magma storage and extraction associated with plinian and interplinian activity at Santorini Caldera (Greece). *J. Petrol.* 57 (3), 461–494.

Druitt, T.H., McCoy, F.W., Vougioukalakis, G.E., 2019. The Late Bronze Age eruption of Santorini Volcano and its impact on the Ancient Mediterranean World. *Elements: an international magazine of mineralogy. Geochim. Petrol.* 15 (3), 185–190.

Eriksen, U., Friedrich, W., Buchardt, B., Tauber, T., Thomsen, M., 1990. The strongyle caldera: geological palaeontological stable isotope evidence from radiocarbon dated stromatolites from Santorini. In: Hardy, D.A., Dumas, C.G., Sakellaris, J.A., Warren, P.M. (Eds.), *Thera and the Aegean World* III, 2, pp. 139–150.

Evans, K.J., McCoy, F., 2020. Precursory eruptive activity and implied cultural responses to the Late Bronze Age (LBA) eruption of Thera (Santorini, Greece). *J. Volcanol. Geotherm. Res.* <https://doi.org/10.1016/j.jvolgeores.2020.106868>.

Fabbro, G.N., Druitt, T.H., Scaillet, S., 2013. Evolution of the crustal magma plumbing system during the build-up to the 22-ka caldera-forming eruption of Santorini (Greece). *Bull. Volcanol.* 75, 767.

Flaherty, T., Druitt, T., Tuffen, H., Higgins, M.D., Costa, F., Cadoux, A., 2018. Multiple time-scale constraints for high-flux magma chamber assembly prior to the Late Bronze Age eruption of Santorini (Greece). *Contrib. Mineral. Petrol.* 173 (9), 75.

Fouqué, F., 1879. In: Masson, G. (Ed.), *Santorini et ses Eruptions*. Librairie l'Académie de Médecine, Paris (440 p).

Friedrich, W.L., 2000. *Fire in the Sea: The Santorini Volcano, Natural History and the Legend of Atlantis*. Cambridge University Press (258 p).

Friedrich, W.L., Eriksen, U., Tauber, H., Heinemeier, J., Rud, N., Thomsen, M., Buchardt, B., 1988. Existence of a water-filled caldera prior to the Minoan eruption of Santorini, Greece. *Naturwissenschaften* 75 (11), 567–569.

Friedrich, W.L., Kromer, B., Friedrich, M., Heinemeier, J., Pfeiffer, T., Talamo, S., 2006. Santorini eruption radiocarbon dated to 1627–1600 BC. *Science* 312 (5773), 548.

Fytikas, M., Vougioukalakis, G., 2005. The South Aegean Active Volcanic Arc: Present Knowledge and Future Perspectives. Elsevier.

Gertisser, R., Preece, K., Keller, J., 2009. The Plinian Lower Pumice 2 eruption, Santorini, Greece: magma evolution and volatile behaviour. *J. Volcanol. Geotherm. Res.* 186 (3–4), 387–406.

Heiken, G., McCoy, F., 1984. Caldera development during the Minoan eruption, Thira, Cyclades, Greece. *J. Geophys. Res. Solid Earth* 89 (B10), 8441–8462.

- Heiken, G., McCoy, F., 1990. Precursory activity to the Minoan eruption, Thera, Greece. In: Hardy, D.A., Doumas, C.G., Sakellaris, J.A., Warren, P.M. (Eds.), *Thera and the Aegean World III*. 2, pp. 79–88.
- Höflmayer, F., 2012. The date of the Minoan Santorini eruption: quantifying the “offset”. *Radiocarbon* 54 (3–4), 435–448.
- Hooft, E., Heath, B., Toomey, D., Paulatto, M., Papazachos, C., Nomikou, P., Morgan, J., Warner, M., 2019. Seismic imaging of Santorini: subsurface constraints on caldera collapse and present-day magma recharge. *Earth Planet. Sci. Lett.* 514, 48–61.
- Hope Simpson, R., Dickinson, O.T.P.K., 1979. A gazetteer of Aegean civilisation in the Bronze Age. 1. The mainland and the islands. *Studies in Mediterranean Archaeology*. 52. Åström (430 p).
- Johnston, E., Sparks, R., Phillips, J., Carey, S., 2014. Revised estimates for the volume of the Late Bronze Age Minoan eruption, Santorini, Greece. *J. Geol. Soc.* 171 (4), 583–590.
- Johnston, E., Sparks, R., Nomikou, P., Livanos, I., Carey, S., Phillips, J., Sigurdsson, H., 2015. Stratigraphic relations of Santorini's intracaldera fill and implications for the rate of post-caldera volcanism. *J. Geol. Soc.* 172 (3), 323–335.
- Karátson, D., Gertisser, R., Telbisz, T., Vereb, V., Quidelleur, X., Druitt, T., Nomikou, P., Kósik, S., 2018a. Reconstructing the Late Bronze Age intra-caldera island of Santorini, Greece. In: Corsaro, R.A., Di Giuseppe, M.G., Isaia, R., Mormone, A., Nave, R. (Eds.), *Abstracts Volume of the International Meeting Cities on Volcanoes 10, "Millenia of Stratification between Human Life and Volcanoes: Strategies for Coexistence"* (Naples, Italy).
- Karátson, D., Gertisser, R., Telbisz, T., Vereb, V., Quidelleur, X., Druitt, T., Nomikou, P., Kósik, S., 2018b. Towards reconstruction of the lost Late Bronze Age intra-caldera island of Santorini, Greece. *Sci. Rep.* 8 (1), 7026.
- Kockel, V., Schütze, S., 2016. *Fausto and Felice Niccolini. The Houses and Monuments of Pompei*. Taschen (648 p).
- Kutschera, W., 2020. On the enigma of dating the Minoan eruption of Santorini. *PNAS* 117 (16), 8677–8679. <https://doi.org/10.1073/pnas.2004243117>.
- Manning, S., 2014. A Test of Time and a Test of Time Revisited. The Volcano of Thera and the Chronology and History of the Aegean and East Mediterranean in the Mid-second Millennium BC, *Oxbow*, Oxford.
- Manning, S.W., Kromer, B., Cremaschi, M., Dee, M.W., Friedrich, R., Griggs, C., Hadden, C.S., 2020. Mediterranean radiocarbon offsets and calendar dates for prehistory. *Sci. Adv.* 6 (12), eaaz1096. <https://doi.org/10.1126/sciadv.aaz1096>.
- Marinatos, S., 1939. The volcanic destruction of Minoan Crete. *Antiquity* 13 (52), 425–439.
- Marinatos, S., 1967–1974. *Excavations at Thera I–VII*. The Archaeological Society of Athens, Athens.
- McAneney, J., Baillie, M., 2019. Absolute tree-ring dates for the Bronze Age eruptions of Aniakhchak and Thera in light of a proposed revision of ice-core chronologies. *Antiquity* 99 (367), 99–112.
- McClelland, E., Thomas, R., 1990. A palaeomagnetic study of Minoan age tephra from Thera. In: Hardy, D.A., Doumas, C.G., Sakellaris, J.A., Warren, P.M. (Eds.), *Thera and the Aegean World III*. 2, pp. 129–138.
- Morris, S.P., 1989. A tale of two cities: the miniature frescoes from Thera and the origins of Greek poetry. *Am. J. Archaeol.* 511–535.
- Morris, S.P., 2000. From Thera to Scheria: Aegean art and narrative. *The Wall Paintings of Thera: Proceedings of the First International Symposium*, pp. 317–333.
- Newhall, C., Self, S., Robock, A., 2018. Anticipating future Volcanic Explosivity Index (VEI) 7 eruptions and their chilling impacts. *Geosphere* 1–32.
- Nomikou, P., Papanikolaou, D., Alexandri, M., Sakellariou, D., Rousakis, G., 2013. Submarine volcanoes along the Aegean Volcanic Arc. *Tectonophysics* 507–508, 123–146.
- Nomikou, P., Parks, M.M., Papanikolaou, D., Pyle, D.M., Mather, T.A., Carey, S., Watts, A.B., Paulatto, M., Kalnins, M.L., Livanos, I., Bejelou, K., Simou, E., Perros, I., 2014. The emergence and growth of a submarine volcano: the Kameni islands, Santorini (Greece). *Geo. Res. J.* 1–2, 8–18.
- Nomikou, P., Druitt, T., Hübscher, C., Mather, T., Paulatto, M., Kalnins, L., Kelfoun, K., Papanikolaou, D., Bejelou, K., Lampridou, D., 2016. Post-eruptive flooding of Santorini caldera and implications for tsunami generation. *Nat. Commun.* 7, 13332.
- Palyvou, C., 2005. *Akrotiri, Thera: An Architecture of Affluence 3,500 Years Old*. INSTAP Academic Press.
- Papazachos, B., Comninakis, P., 1971. Geophysical and tectonic features of the Aegean arc. *J. Geophys. Res.* 76 (35), 8517–8533.
- Pearson, C.L., Brewer, P.W., Brown, D., Heaton, T.J., Hodgins, G.W., Jull, A.T., Lange, T., Salzer, M.W., 2018. Annual radiocarbon record indicates 16th century BCE date for the Thera eruption. *Sci. Adv.* 4 (8), eaar8241.
- Pfeiffer, T., 2001. Vent development during the Minoan eruption (1640 BC) of Santorini, Greece, as suggested by ballistic blocks. *J. Volcanol. Geotherm. Res.* 106 (3–4), 229–242.
- Pichler, H., Kussmaul, S., 1972. The calc-alkaline volcanic rocks of the Santorini Group (Aegean Sea, Greece). *Neues Jb. Mineral. Abh.* 116, 268–307.
- Pyle, D.M., 1990. New estimates for the volume of the Minoan eruption. In: Hardy, D.A., Doumas, C.G., Sakellaris, J.A., Warren, P.M. (Eds.), *Thera and the Aegean World III*. 2, pp. 113–121.
- Rehak, P., Younger, J.G., 1998. Review of Aegean prehistory VII: neopalatial, final palatial, and Postpalatial Crete. *Am. J. Archaeol.* 102 (1), 91–173.
- Sakellariou, D., Roussakis, G., Nomikou, P., Croff Bell, K., Carey, S., Sigurdsson, H., 2012. Tsunami triggering mechanisms associated with the 17th cent. BC Minoan eruption of Thera volcano, Greece. *Proceedings of the International Offshore and Polar Engineering Conference*, p. 61.
- Sigurdsson, H., Carey, S., Devine, J., 1990. Assessment of mass, dynamics and environmental effects of the Minoan eruption of Santorini volcano. In: Hardy, D.A., Doumas, C.G., Sakellaris, J.A., Warren, P.M. (Eds.), *Thera and the Aegean World III*. 2, pp. 100–112.
- Sigurdsson, H., Carey, S., Alexandri, M., Vougioukalakis, G., Croff, K., Roman, C., Sakellariou, D., Anagnostou, C., Rousakis, G., Ioakim, C., 2006. Marine investigations of Greece's Santorini volcanic field. *EOS Trans. Am. Geophys. Union* 87 (34), 337–342.
- Siklós, Z., Demény, A., Vennemann, T.W., Pilet, S., Kramers, J., Leél-Össey, S., Bondár, M., Shen, C.C., Hegner, E., 2009. Bronze Age volcanic event recorded in stalagmites by combined isotope and trace element studies. *Rapid Commun. Mass Spectrom.* 23 (6), 801–808.
- Spakman, W., Wortel, M., Vlaar, N., 1988. The Hellenic subduction zone: a tomographic image and its geodynamic implications. *Geophys. Res. Lett.* 15 (1), 60–63.
- Strahler, A.N., 1957. Quantitative analysis of watershed geomorphology. *EOS Trans. Am. Geophys. Union* 38 (6), 913–920.
- Strasser, T.F., 2010. Location and perspective in the Thera Flotilla Fresco. *J. Mediterr. Archaeol.* 23 (1), 3–26.
- Strasser, T.F., Chapin, A.P., 2014. Geological formations in the Flotilla Fresco from Akrotiri. In: Touchais, G., Laffineur, R., Rougemont, F. (Eds.), *Physis: l'environnement naturel et la relation homme-milieu dans le monde égéen protohistorique*. *Aegaeum* 37, pp. 57–64.
- Tsonis, A., Swanson, K., Sugihara, G., Tsonis, P., 2010. Climate change and the demise of Minoan civilization. *Clim. Past* 6 (4), 525–530.
- Vassilopoulos, A., Evelpidou, N., Chartidou, K., 2009. Vassilopoulos A. Geomorphological evolution of Santorini. In: Evelpidou, N., de Figueiredo, T., Mauro, F., Tecim, V., Vassilopoulos, A. (Eds.), *Natural Heritage from East to West. Case Studies from 6 EU Countries*. Springer, pp. 1–14.
- Vereb, V., 2016. A Santorini vulkán minósi kitoréstermékeinek fotóstatistikai és térinformatikai elemzése (Photo-statistical and GIS Analysis of the Minoan Products of Santorini Volcano: in Hungarian). MSc thesis. Eötvös University (75 p).
- Vinther, B.M., Clausen, H.B., Johnsen, S.J., Rasmussen, S.O., Andersen, K.K., Buchardt, S.L., Dahl-Jensen, D., Seierstad, I.K., Siggaard-Andersen, M.L., Steffensen, J.P., 2006. A synchronized dating of three Greenland ice cores throughout the Holocene. *J. Geophys. Res. Atmos.* 111 (D13102).
- Wachsmann, S., 1998. *Seagoing Ships and Seamanship in the Bronze Age Levant* (College Station, Texas).
- Wagstaff, J.M., 1978. A possible interpretation of settlement pattern evolution in terms of a catastrophe theory. *Trans. Inst. Brit. Geogr.* NS (3), 165–178.
- Warren, P., 1979. The Miniature Fresco from the West House at Akrotiri, Thera, and its Aegean setting. *J. Hell. Stud.* 99, 115–129.
- Warren, P., Czerny, E., Hein, I., Hunger, H., Melman, D., Schwab, A., 2006. The date of the Thera eruption in relation to Aegean-Egyptian interconnections and the Egyptian historical chronology. *Timelines: Studies in Honour of Manfred Bietak*. 2, pp. 305–321.
- Watkins, N., Sparks, R., Sigurdsson, H., Huang, T., Federman, A., Carey, S., Ninkovich, D., 1978. Volume and extent of the Minoan tephra from Santorini Volcano: new evidence from deep-sea sediment cores. *Nature* 271 (5641), 122.
- Wayland-Barber, E., Barber, P.T., 2006. *When they Severed Earth from Sky: How the Human Mind Shapes Myth*. Princeton University Press (312 p).
- Wiener, M.H., 2009. The state of the debate about the date of the Thera eruption. *Time's up: 197–206*. In: Warburton, D.A. (Ed.), *Time's up! Acts of the Minoan Eruptive Chronology Workshop, Sandbjerg, November 2007*. Monographs of the Danish Institute at Athens vol. 10. Aarhus University Press, pp. 197–206.
- Wohletz, K., Brown, W., 1995. Particulate size distributions and sequential fragmentation/transport theory. *Proceedings of US (NSF) Japan (JSPS) Joint Seminar, Santa Barbara, CA*, pp. 235–241.
- Wulf, S., Keller, J., Satow, C., Gertisser, R., Kraml, M., Grant, K.M., Appelt, O., Vakhrameeva, P., Koutsodendris, A., Hardiman, M., 2020. Advancing Santorini' ~360 kyrs. *Earth Sci. Rev.* 200, 102964.